NINETEENTH EUROPEAN ROTORCRAFT FORUM

Paper No. B9

NUMERICAL INVESTIGATION OF THE BASIS MECHANISMS OF BVI-NOISE GENERATION

by

K. Ehrenfried, G.E.A. Meier

DLR Göttingen, Germany

September 14 – 16, 1993
CERNOBBIO (Como)
ITALY

ASSOCIAZIONE INDUSTRIE AEROSPAZIALI
ASSOCIAZIONE ITALIANA DI AERONAUTICA ED ASTRONAUTICA

NUMERICAL INVESTIGATION OF THE BASIC MECHANISMS OF BVI-NOISE GENERATION

by K. Ehrenfried and G.E.A. Meier

DLR Institute of Experimental Fluid Mechanics,
Göttingen, Germany

Abstract

Two-dimensional vortex-airfoil interactions are investigated numerically by solving the unsteady Euler equations using a finite-volume scheme. The computational domain is extended up to 10 cord length away from the airfoil and non-reflecting conditions are applied at the outer boundary. This allows to investigate the propagation of the generated sound waves and the determination in which directions the strongest waves are emitted. The calculations yield a direct connection between the processes directly at the airfoil and the form of the emitted sound waves. The influence of the airfoil geometry and other parameters on these wave forms is discussed.

1. Introduction

In previous works the two-dimensional vortex-airfoil interaction as a model for the blade-vortex interaction was already investigated numerically and experimentally (see references 1 to 6). The processes, which occur during the interaction close to the airfoil, were studied in detail. Main results of these investigations are that several mechanisms of sound generation may be effective. Most important is the emission of the so called *compressibility wave* and the *transonic wave*. The first one is generated at the nose of the airfoil as result of a temporary increase of the stagnation pressure connected with a movement of the stagnation point. The second wave occurs if a supersonic region arises temporarily between the airfoil and the vortex core. As shown in reference 2 the generation of such a supersonic region depends on the free stream Mach number and the induced velocity of the vortex. The supersonic region is bounded by a shock wave which finally is emitted as a strong sound wave. This happens when the vortex separates from the shock wave and the supersonic region breaks down. Recent investigations show that some mechanisms at the trailing edge of the airfoil also generate pressure waves, when the vortex passes the trailing edge.

One question which arises from all the previous studies is how the generated waves propagate away from the airfoil and which fluctuations in the far field occur. The experimental techniques are restricted to a close region around the airfoil and don't allow to observe far field effects. Thus the numerical calculations were modified to cover an extended domain which reaches up to 10 cord length away from the airfoil. This is of course not the true far field,

but the calculations give an idea what the emitted waves look like further away from their origin. To obtain undisturbed results non-reflecting boundary conditions are applied at the outer boundary. To investigate the waves in the outer region the numerical scheme must be able to handle relative weak sound waves and strong effects like the shock waves which occur at the airfoil. Therefore a higher order discretisation with reduced numerical dissipation is absolutely necessary. More details about the numerical method are given in the next section. In section 3 some numerical results are presented and the influence of some parameters on the sound generation is investigated. One parameter of interest is the airfoil geometry. Calculation were done with NACA0012 and NACA23012 airfoils. Another important parameter beside the Mach number is the so called *miss distance*. This parameter is defined as the initial displacement of the vortex center from the line, which is parallel to the free flow direction and passes directly through the quarter-cord point. So the miss distance determines the distance at which the vortex passes the airfoil. Due to the limited space only calculations with Mach number $Ma = 0.8$ and zero angle of attack are presented in this paper.

2. Numerical procedure

A finite-volume scheme which works on unstructured grids is used to solve the unsteady Euler equations. The numerical flux is calculated using flux-difference splitting with Osher's approximate Riemann solver. A higher order spatial interpolation is used to reduce the numerical dissipation. Otherwise the incoming vortex and the generated sound waves would be damped in an unrealistic way and the results would be disturbed. To avoid unphysical oscillations in regions with strong gradients a special flux limiter is applied. More details of the numerical method are given in reference 4.

In figure 1 the pressure distribution of a typical initial condition is shown. In this example a NACA0012 airfoil is used. At the beginning of the calculation the flow around the airfoil equals the steady solution with the exception that upstream of the airfoil a vortex is inserted in the flow. This vortex simply moves with the free flow towards the airfoil until the actual interaction starts and the flow field becomes unsteady to a large extent. The special procedure to calculate this initial condition is explained in reference 4 and 5. In the presented examples a vortex with circulation $\Gamma = 1.21$ and core radius $r_{core} = 0.25L$ is used. Here L is the cord length and the circulation is normalized with L and the free stream velocity u_∞.

Figure 1 shows the complete computational domain. The solution is computed on a grid with more than 16,000 points. To give an idea of the spatial resolution a section of the grid around the airfoil is depicted in figure 2. At the rigid wall of the airfoil a simple 'no flow through' condition is used. At the outer boundary a more complex non-reflecting condition is applied. The implemented condition is based on the theory presented by Giles in reference 7.

3. Numerical results

First of all an example with a NACA23012 airfoil is considered. Figure 3 shows a time series of pressure distributions in a section around the airfoil during the interaction. The given time t is normalized with the cord length L and a normal velocity v_{norm} which is defined by the stagnation value of pressure p_0 and density ρ_0 in the free flow:

$$t_{norm} = L/v_{norm}; \qquad v_{norm} = \sqrt{p_0/\rho_0}.$$

The vortex rotates in clockwise direction and the miss distance is $\Delta y = 0.25$ This is a typical configuration as it occurs at real blade-vortex interactions. The first frame shows the approaching vortex with its center still more than one cord length away. At this time the flow around the airfoil is relatively undisturbed by the vortex. A strong shock wave is present at the upper side of the airfoil. For the given Mach number $Ma = 0.8$ the flow at the lower side is close to transonic conditions but only a small sign of the beginning of a shock wave is visible. For the given geometry a steady shock wave exists on the lower side only at higher Mach numbers. The flow acceleration, which is induced by the vortex, generates immediately a supersonic region on the lower side when the vortex comes closer to the airfoil. This is visible at $t = 3.0$. The generated supersonic region is bounded by a strong shock wave and the whole structure consisting of supersonic region, shock wave and vortex is driven by the mean flow along the airfoil in downstream direction.

The induced velocity has changed the flow field in the nose region of the airfoil too. Between $t = 1.5$ and $t = 3.0$ the stagnation pressure increases about more than 50% and the stagnation point moves towards the upper side. Later, after the vortex has passed and the induced velocity has decreased in this region, the stagnation point travels temporarily to the lower side and then back to its initial position. During this process the pressure in the stagnation point goes back to the initial value. The unsteady pressure fluctuation in the nose region causes the emission of a compression wave, the so called *compressibility wave*. This wave is clearly visible in following frames $t = 3.5$ and later. It travels in upstream direction independently of the other processes which take place around the airfoil.

At a certain time the vortex separates from the supersonic region and the shock wave at the lower side. This happens very suddenly and the supersonic region breaks down immediately. The remaining shock wave is weakened and it starts to travel in upstream direction. Further calculations have shown, that the position at which this separation of vortex, supersonic region and shock wave takes place is mainly determined by the *miss distance*. If the vortex center is closer to the airfoil the separation takes place earlier. This is important for the force and momentum fluctuations during the interaction. In the supersonic region relative low pressure is present. Especially if this region is driven along the lower side close to the trailing edge it has a strong influence on the momentum with respect to the quarter-cord point.

From an acoustic point of view the breakdown of the supersonic region causes the release of a shock wave which travels in upstream direction along the lower side. Later it leaves the airfoil and follows the first compression wave. This second wave is called *transonic wave*. In addition to these two main effects more sound waves are generated when the vortex passes the trailing edge of the airfoil. This is visible for $t = 4.0$ and $t = 4.5$. At first a compression wave on the upper side is generated which then travels in upstream direction and merges with the initial shock wave. With a little delay a further compression wave occurs on the lower side. This wave travels in upstream direction and follows the transonic wave.

In contrast to the process on the lower side the initial shock wave on the upper side is relative weakly influenced by the interaction. It is slightly deformed and the shock foot moves slowly towards the trailing edge during the beginning of the interaction. The compression wave from the trailing edge is too weak to have a strong influence on the main shock. So the main shock simply moves slowly back to its initial position after the interaction has been finished. All the calculated effects and mechanisms in the area close to the airfoil are confirmed by experimental observations. Also the additional waves from the trailing edge were proved in recent experiments.

To investigate how the generated waves propagate in the outer regions the solution in the whole computational domain is regarded. Because the sound waves become very weak, not the pressure itself but the pressure variation

$$p'(x, y, t) = p(x, y, t) - p_{steady}(x, y)$$

is depicted in figure 4 for $t = 10.0$. At this time the vortex is already 5 cord lengths downstream of the airfoil. The generated waves form circular wave fronts with the vortex at its center. At first we regard all phenomena in a reference frame which moves with mean flow velocity downstream. In this reference frame the vortex has a fixed position and the airfoil moves and passes the vortex. For simplicity we assume that the coordinate system of the moving reference frame has the same orientation as the one for the fixed reference frame. Then the airfoil moves in negative x-direction. For low Mach numbers one would expect a dipole like sound generation by this process. The orientation of the dipole is so that the main sound is emitted in the direction normal to the path of the airfoil, namely in y-direction. The direction of rotation of the vortex determines the sign of the emitted waves. In the following a clockwise rotating vortex is assumed. Below of the vortex at $y < 0$ one observes first a pressure decrease then an increase above the initial value followed by a decrease back to the initial value. On the side above the vortex ($y > 0$) the sign of the pressure fluctuation is simply inverted.

In the presented case with Mach number $Ma = 0.8$ we get a deviation from the ideal dipole. In principle the calculated sign of the pressure waves corresponds to a dipole field, but the form of the dipole is distorted. The calculated wave front has its largest amplitude not directly normal to the x-axis but in oblique directions which are slightly rotated towards the

direction of motion of the airfoil. Strong amplitudes occur in the wave front even directly in the direction of motion. From acoustic theory which holds for low Mach numbers one would expect minimum emission in this direction. It seems that the nonlinear effects in the transonic flow field cause some additional – let say 'higher order' – waves besides a dipole like emission. These waves occur as separate maxima in the wave front mainly close to the direction of the airfoil movement. In fact these waves can be identified as the *compressibility wave* and the *transonic wave*. Their generation mechanisms were already explained above with figure 3.

In the reference frame which is fixed to the airfoil and the computational grid the main sound is emitted in downstream directions. This is due to the convection of the sound field by the mean flow. Figure 5 tries to visualize the development of the sound waves. In the contour plot the value of

$$p'_{max}(x,y) = \max_{0<t<t_{end}} p'(x,y,t)$$

is shown, where the computation was done up to $t_{end} = 15.0$. Here only the pressure waves with positive amplitude were taken into account. But this representation gives an idea how the amplitudes decrease while the wave front propagates away from the airfoil. Along each contour line the observed maximum pressure amplitude is constant. The lines are draw for the values of $p'_{max} = 0.005,\ 0.01,\ 0.015, \ldots$.

To investigate the influence of the airfoil geometry figure 6 shows the same as figure 4 but for a calculation with NACA0012 airfoil. The resulting wave fronts look very similar. Also the magnitude of the pressure fluctuations is nearly the same in both cases. The main difference occurs in the region upstream of the leading edge, where the part of the wave front related to the *transonic wave* is much weaker than in the case of the NACA23012 airfoil. This can be explained by the differences in the steady solutions around both airfoils. In contrast to the NACA23012 the NACA0012 is a symmetric airfoil. At Mach number $Ma = 0.8$ the steady flow around NACA0012 has two symmetric shock waves on the airfoil. Thus the main difference is an initial shock wave at the lower side. At the beginning of the interaction very similar processes occur on the lower side of both airfoils. In the case of the NACA0012 the vortex also generates a supersonic region bounded by a shock wave. But now this new shock merges with the initial one when the vortex drives the supersonic region along the lower side. Later, after the vortex separates from the supersonic region, the released shock wave is not able to leave the airfoil. It simply swings back to its initial position while always a supersonic region is present. Additionally the wave which is generated at the trailing edge is hindered by the main shock wave to travel along the lower side and leave the airfoil. Of course the motion of the shock wave on the lower side causes an emission of sound waves but especially the *transonic wave* is not generated like in the case of NACA23012.

The comparison of the solutions for NACA23012 and NACA0012 shows how the airfoil geometry influences the generated sound field. In the following the influence of the *miss distance* is considered. Therefore a calculation with NACA0012 airfoil and miss distance $\Delta y =$

0 is presented. This means that the vortex core hits directly the nose of the airfoil. The contour plot of the pressure variation at $t = 10.0$ for this case is depicted in figure 7. At first sight the generated waves seem similar to the examples shown above. The main difference is the form of the wave fronts which propagate approximately in upstream direction. In some directions stronger sound waves are emitted and in other direction the emitted waves are weaker. Thus no general statement can be made in which of the presented examples more sound is generated. Like in the case of $\Delta y = 0.25$ the pattern of the pressure fluctuations has roughly the typical dipole like form. But both the *compressibility wave* and the *transonic wave* can not be observed in figure 7. Indeed in the case of zero miss distance none of these waves is generated at all.

4. Conclusions

The extended computational domain allows to investigate the development of the sound waves which were generated by the vortex airfoil interaction. The compression waves, which are generated due to compressibility and transonic effects, are clearly visible as deviations from a more or less dipole like sound generation. A direct assignment of the waves, which occur during the interaction in the near field, and parts of the wave fronts at later times can be made.

Of course the presented three examples cover only a very small area of possible configurations. So the results can only give an idea of the possible effects which may occur at vortex-airfoil interaction. Considering the presented comparison between NACA0012 and NACA23012 it seems that the airfoil geometry has a rather weak influence on the generated sound. In this context one has to take into account that both airfoils have the same maximum thickness of 12% of the cord length. From these results one can not expect that a significant reduction of the generated sound can be achieved by minor changes in the airfoil geometry. Further the presented results show that the *miss distance* is a very important parameter which has a clear influence on the generated sound waves. If it is possible to manipulate the *miss distance* in the case of the real blade-vortex interaction one has probably an effective way to favorably influence the sound generation. Further investigations have to be made to evaluate the dependency on this parameter in detail.

5. References

1. H.-M. Lent, K.F. Löhr, G.E.A. Meier and U. Schievelbusch, "Some processes of sound generation in a vortex-airfoil system with parallel axes", J. Acoustique 2, 365-367 (1989)
2. G.E.A. Meier, U. Schievelbusch and H.-M. Lent, "Stoßwellenentstehung bei transsonischer Wirbel-Profil-Wechselwirkung", Z. Flugwiss. Weltraumforsch., Vol. 14 (1990), pp 327-332.

3. H.-M. Lent, G.E.A. Meier, F. Obermeier, U. Schievelbusch, O. Schürmann, "Noise Mechanisms of transonic Blade-Vortex-Interaction", AIAA Paper 90-3972, 13th Aeroacoustics Conference, Tallahassee, Florida, 22.-24. October 1990.

4. K. Ehrenfried, "Numerische Untersuchung von Wirbel-Tragflügel-Wechselwirkungen im transsonischen Geschwindigkeitsbereich", MPI für Strömungsforschung Report 8/1991, Göttingen, October 1991.

5. K. Ehrenfried, G.E.A. Meier, F. Obermeier, K.-Q. Zhu, "Analytical and Numerical Investigations on Vortex-Airfoil-Interaction", DGLR-AIAA Paper 92-02-020 14th Aeroacoustic Conference, Aachen, Germany, 11.-14. May 1992.

6. H.-M. Lent, G.E.A. Meier, F. Obermeier, O. Schürmann, K.Y. Zhang, "Transonic Blade-Vortex-Interaction Noise: New Experimental Results", DGLR-AIAA Paper 92-02-021 14th Aeroacoustic Conference, Aachen, Germany, 11.-14. May 1992.

7. M.B. Giles, "Non-Reflecting Boundary Conditions for the Euler Equations", Technical Report CFDL-TR-88-1, MIT Computational Fluid Dynamics Laboratory, February 1988.

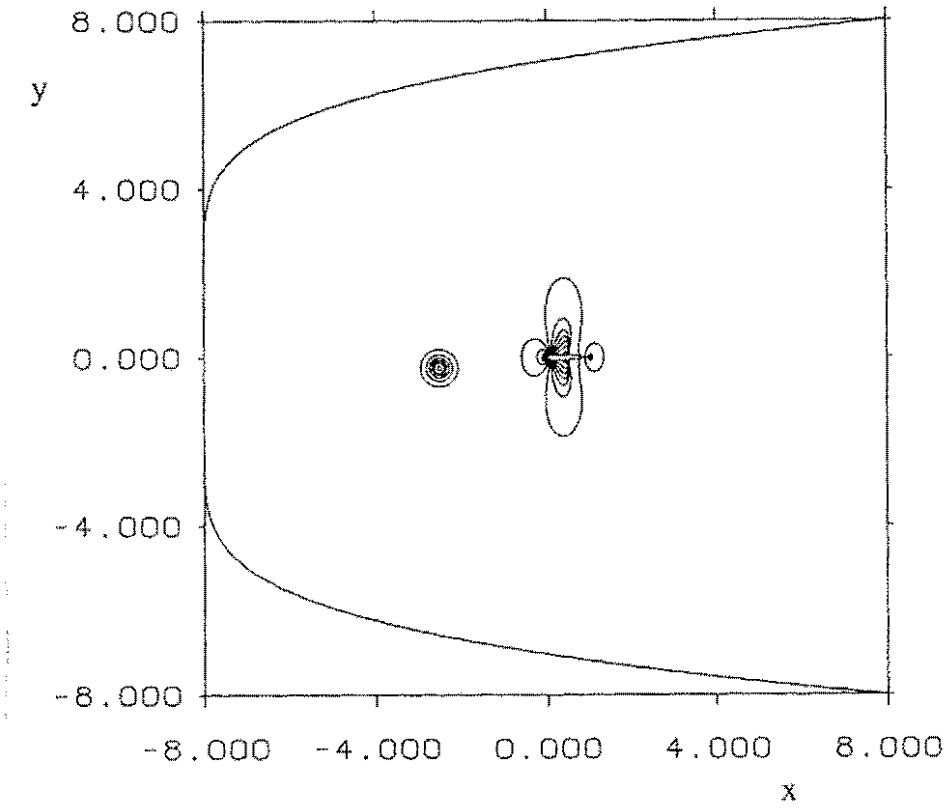

Figure 1: Initial pressure distribution for a calculation with NACA0012 airfoil, Mach number $Ma = 0.8$ and miss distance $\Delta y = 0.25$.

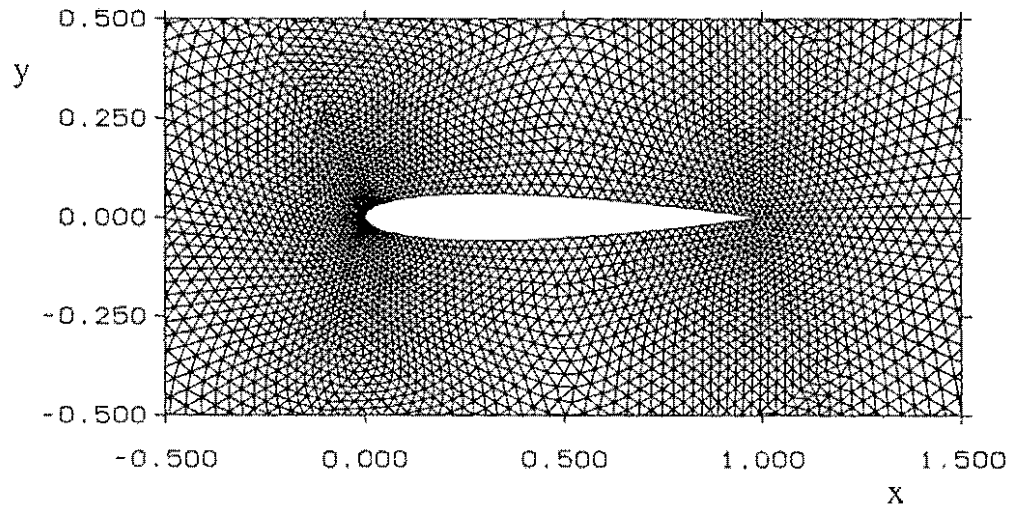

Figure 2: Section of the grid around the NACA0012 airfoil.

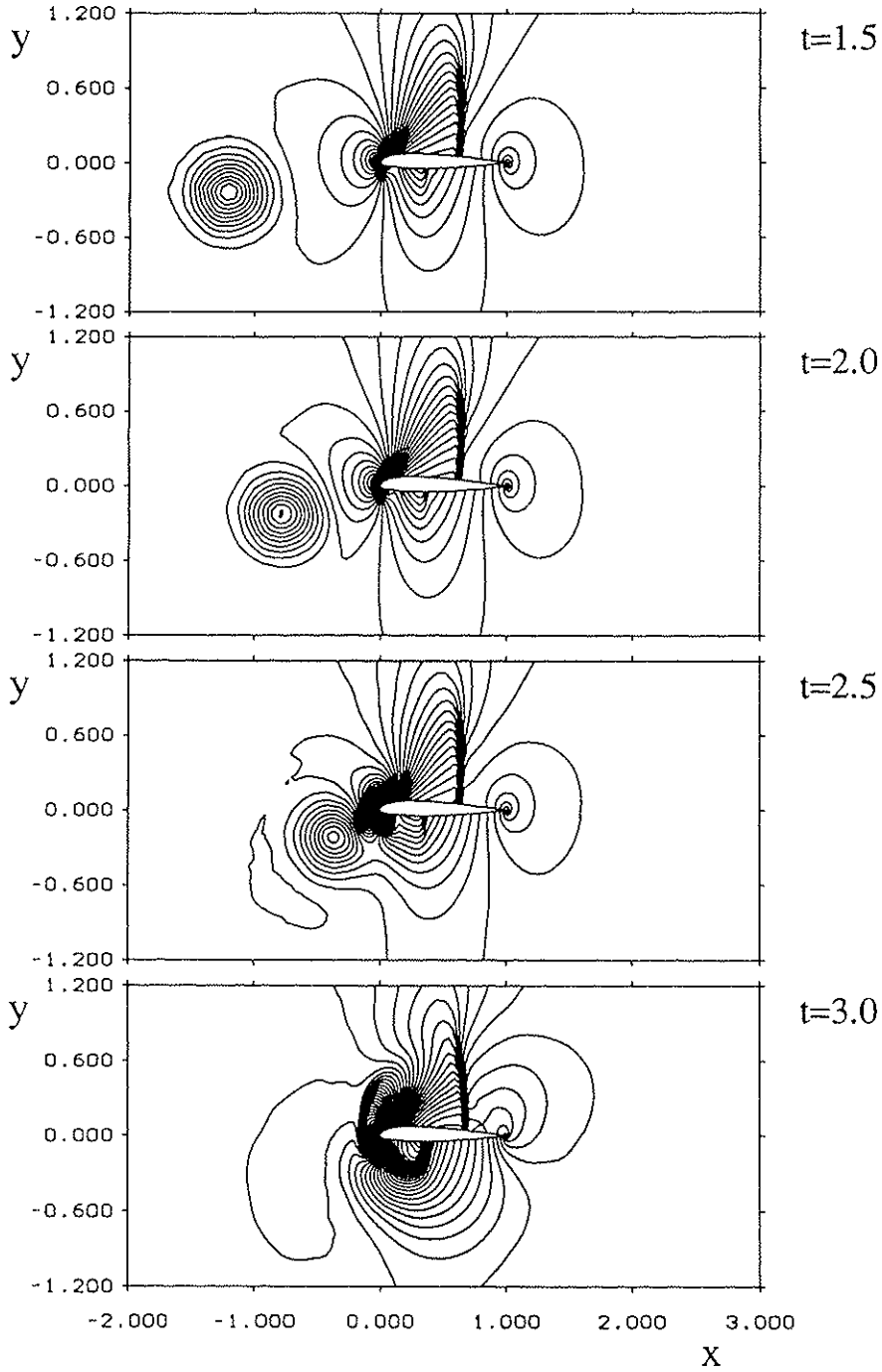

Figure 3: Pressure distribution at various times during the interaction, NACA23012, Mach number $Ma = 0.8$, miss distance $\Delta y = 0.25$ (continued on the next page).

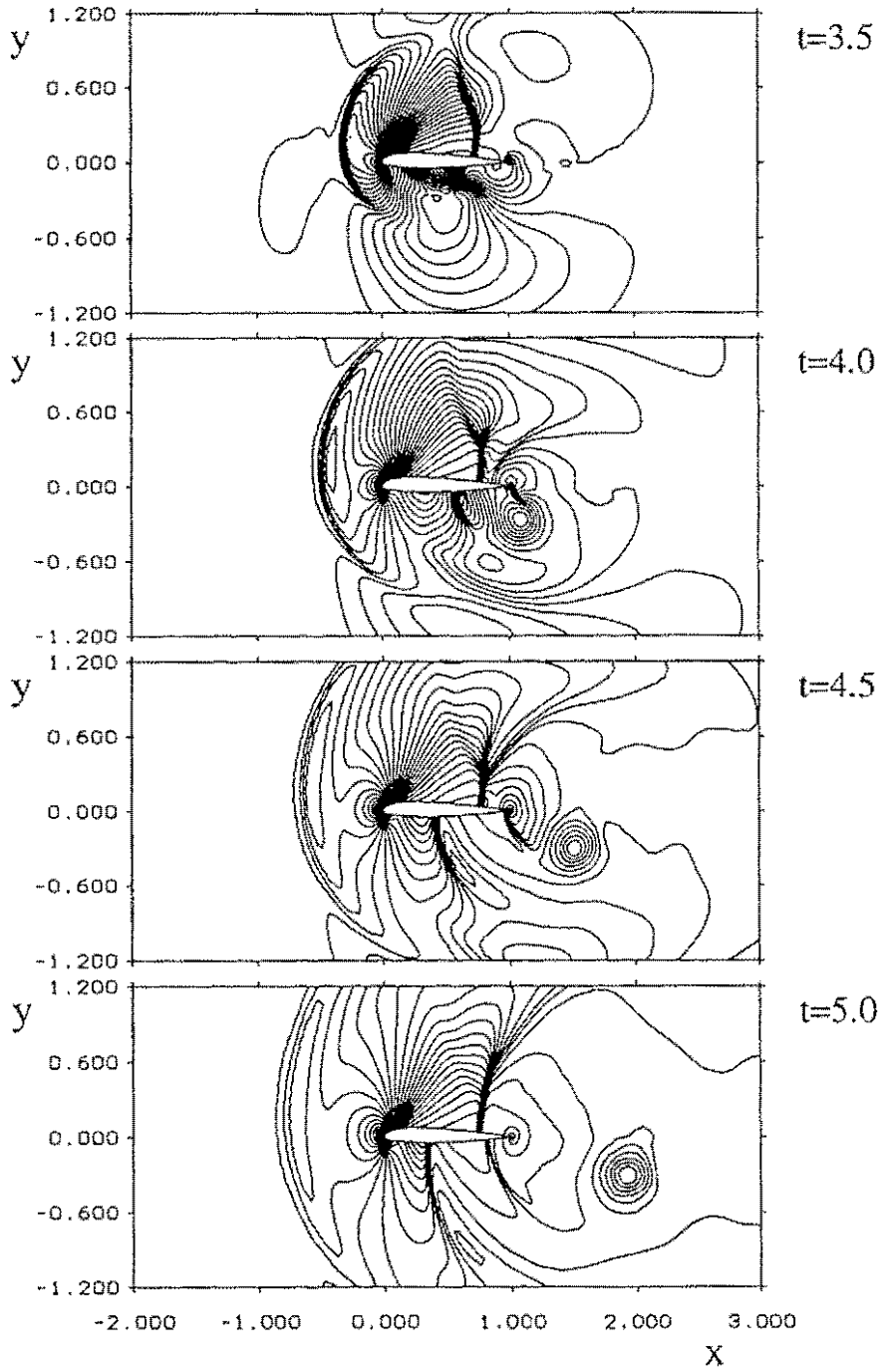

Figure 3: Pressure distribution at various times during the interaction, NACA23012, Mach number $Ma = 0.8$, miss distance $\Delta y = 0.25$ (part two).

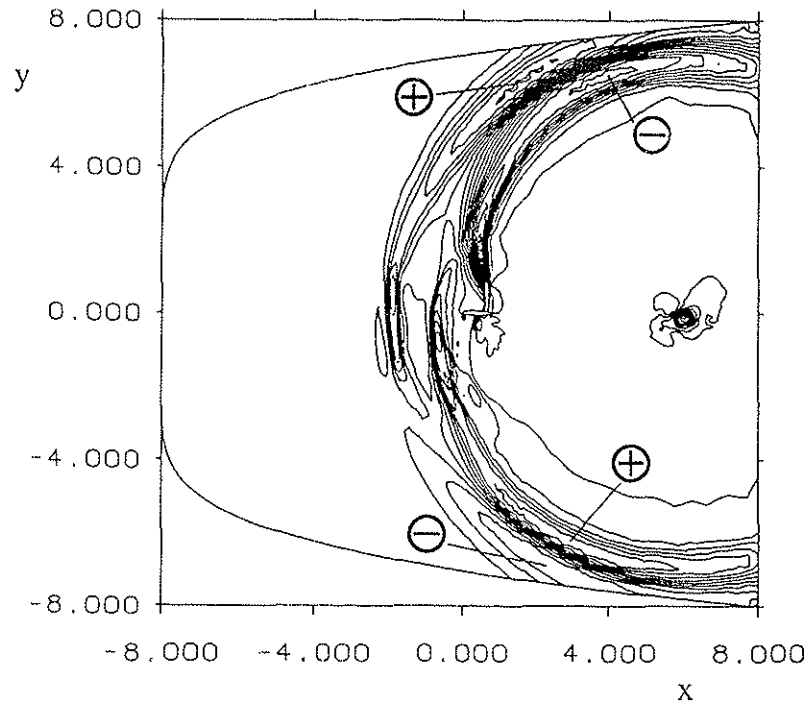

Figure 4: Pressure variation $p'(x, y)$ at $t = 10.0$, NACA23012, Mach number $Ma = 0.8$, miss distance $\Delta y = 0.25$.

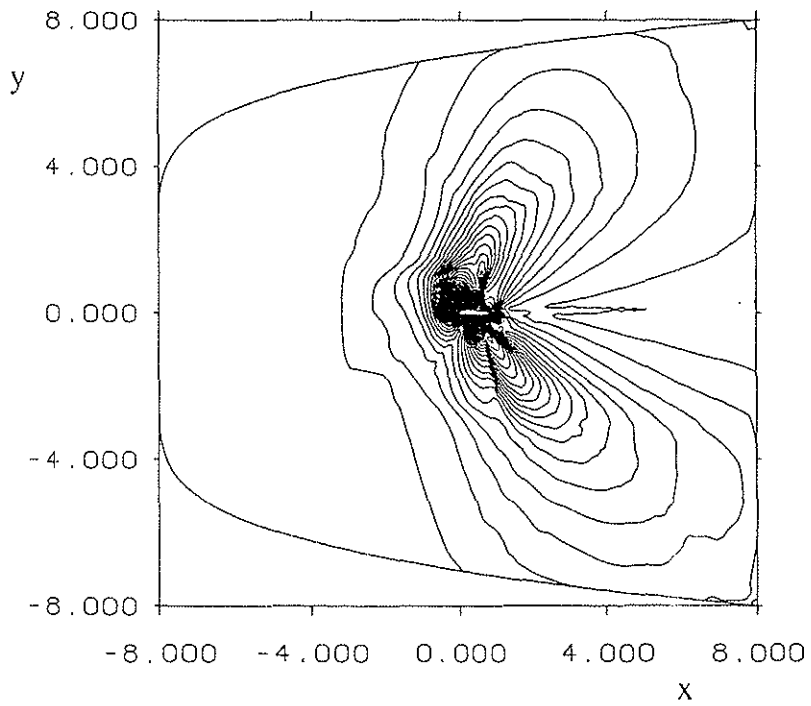

Figure 5: Maximum pressure amplitude $p'_{max}(x, y)$ (see text), NACA23012, Mach number $Ma = 0.8$, miss distance $\Delta y = 0.25$.

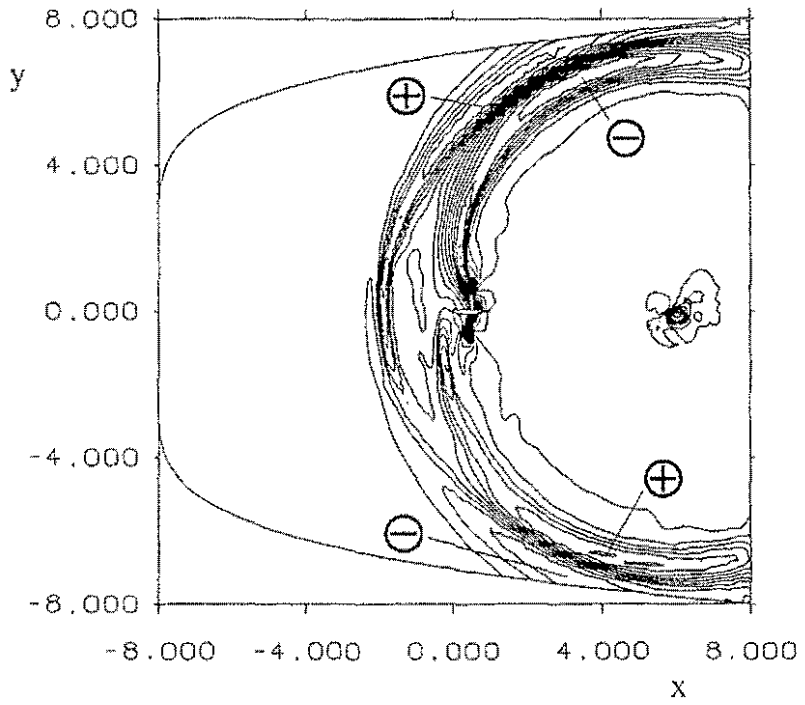

Figure 6: Pressure variation $p'(x, y)$ at $t = 10.0$, NACA0012, Mach number $Ma = 0.8$, miss distance $\Delta y = 0.25$.

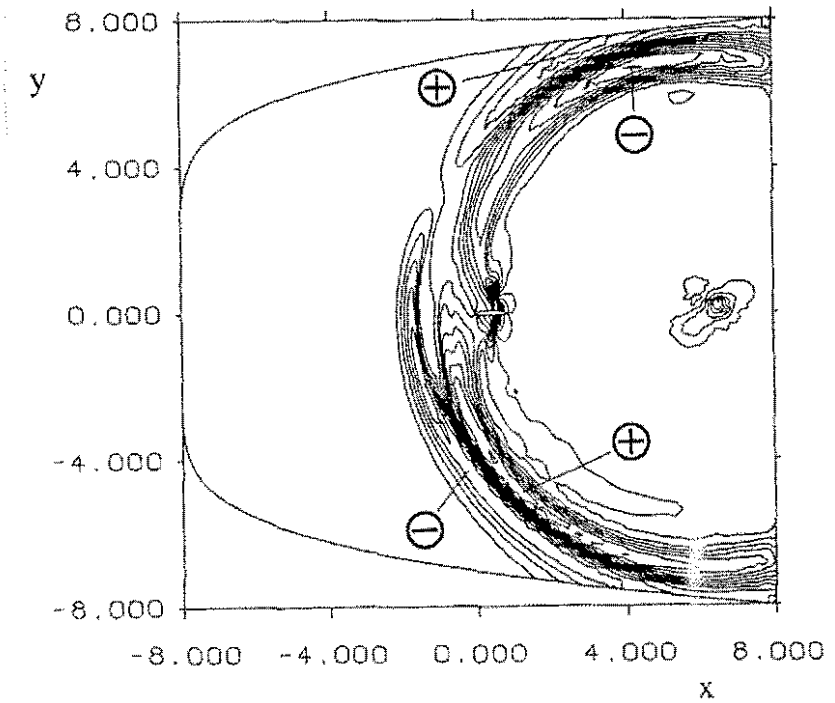

Figure 7: Pressure variation $p'(x, y)$ at $t = 10.0$, NACA0012, Mach number $Ma = 0.8$, miss distance $\Delta y = 0.0$.